Spencer, R., Charman, M., Wilson, P., & Lawson, E. (1976) *Nature (London) 263*, 161–163.
Tarr, G. E. (1986) in *Microcharacterization of Polypeptides: A Practical Manual* (Shively, J. E., Ed.) pp 155–194, Humana, Clifton, NJ.
Trechsel, U., & Fleisch, H. (1981) *FEBS Lett. 135*, 115–118.
Veltmann, J. R., Jr., Jensen, L. S., & Rowland, G. N. (1987) *Nutr. Rep. Int. 35*, 381–392.
Wilbur, W. J., & Lipman, D. J. (1983) *Proc. Natl. Acad. Sci. U.S.A. 80*, 726–730.

^{1}H Fourier Transform NMR Studies of Insulin: Coordination of Ca^{2+} to the Glu(B13) Site Drives Hexamer Assembly and Induces a Conformation Change†

Richard Palmieri,‡,§ Robert W.-K. Lee,‖ and Michael F. Dunn*,‡
Departments of Biochemistry and Chemistry, University of California, Riverside, Riverside, California 92521
Received June 15, 1987; Revised Manuscript Received December 1, 1987

ABSTRACT: ^{1}H Fourier transform NMR investigations of metal ion binding to insulin in ^2H_2O were undertaken as a function of pH* to determine the effects of metal ion coordination to the Glu(B13) site on the assembly and structure of the insulin hexamer. The C-2 histidyl regions of the ^{1}H NMR spectra of insulin species containing respectively one Ca^{2+} and two Zn^{2+}/hexamer and three Cd^{2+}/hexamer have been assigned. Both the Cd^{2+} derivative $(In)_6(Cd^{2+})_2Cd^{2+}$, where two of the Cd^{2+} ions are coordinated to the His(B10) sites and the remaining Cd^{2+} ion is coordinated to the Glu(B13) site [Sudmeier, J. L., Bell, S. J., Storm, M. C., & Dunn, M. F. (1981) *Science (Washington, D.C.) 212*, 560], and the Zn^{2+}–Ca^{2+} derivative $(In)_6(Zn^{2+})_2Ca^{2+}$, where the two Zn^{2+} ions are coordinated to the His(B10) sites and Ca^{2+} ion is coordinated to the Glu(B13) site, give spectra in which the C-2 proton resonances of His(B10) are shifted upfield relative to metal-free insulin. Spectra of insulin solutions (3–20 mg/mL) containing a ratio of $In:Zn^{2+}$ = 6:2 in the pH* region from 8.6 to 10 were found to contain signals both from metal-free insulin species and from the 2Zn–insulin hexamer, $(In)_6(Zn^{2+})_2$. The addition of either Ca^{2+} (in the ratio $In:Zn^{2+}:Ca^{2+}$ = 6:2:1) or 40 mM NaSCN was found to provide sufficient additional thermodynamic drive to bring about the nearly complete assembly of insulin hexamers. Cd^{2+} in the ratio $In:Cd^{2+}$ = 6:3 also drives hexamer assembly to completion. We postulate that the additional thermodynamic drive provided by Ca^{2+} and Cd^{2+} is due to coordination of these metal ions to the Glu(B13) carboxylates of the hexamer. At high pH*, this coordination neutralizes the repulsive Coulombic interactions betwen the six Glu(B13) carboxylates and forms metal ion "cross-links" across the dimer–dimer interfaces. Comparison of the aromatic regions of the ^{1}H NMR spectra for $(In)_6(Zn^{2+})_2$ with $(In)_6(Zn^{2+})_2Ca^{2+}$, $(In)_6(Cd^{2+})_2Cd^{2+}$, and $(In)_6(Cd^{2+})_2Ca^{2+}$ indicates that binding of either Ca^{2+} or Cd^{2+} to the Glu(B13) site induces a conformation change that perturbs the environments of the side chains of several of the aromatic residues in the insulin structure. Since these residues lie on the monomer–monomer and dimer–dimer subunit interfaces, we conclude that the conformation change includes small changes in the subunit interfaces that alter the microenvironments of the aromatic rings.

Insulin is synthesized and stored in the secretory granules of the pancreatic β-cells as a crystalline array of hexamers (Lacy, 1957; Greider et al., 1969; Howell, 1974). The high concentrations of both Zn^{2+} and Ca^{2+} found in these granules (Hellman et al., 1976; Howell et al., 1978; Anderson & Berggren, 1979) and recent studies (Sudmeier et al., 1981; Storm & Dunn, 1985; Dunn et al., 1987; Kaarsholm & Dunn, 1987) strongly suggest these hexamers contain both ions bound to specific sites on the insulin hexamer.

The X-ray diffraction studies of insulin carried out independently in three different countries (Blundell et al., 1972; Bentley et al., 1979; Cutfield et al., 1979, 1981; Peking Insulin Structure Research Group, 1974; Sakabe et al., 1981; Dodson et al., 1979, 1980) have provided refined, high-resolution structures for four different forms of insulin. These forms are respectively the porcine 2Zn–insulin hexamer (Peking Insulin Structure Research Group, 1974; Sakabe et al., 1981; Dodson et al., 1979, 1980; Cutfield et al., 1981; Baker et al., 1987), the porcine 4Zn–insulin hexamer (Bentley et al., 1976; Cutfield et al., 1981; Chothia et al., 1983; Smith et al., 1984), the hagfish metal-free insulin dimer (Cutfield et al., 1979, 1981), and a chemically modified monomeric insulin (Bi et al., 1984; Dong-Cai et al., 1983).

Both the 2Zn and 4Zn hexamers are torus-shaped molecules (Chart I). The insulin subunits are arranged in each hexamer as three symmetry-related insulin dimers about the threefold axis. Because each dimer is asymmetric in the crystal, there are two different subunit conformations in each hexamer. In the 2Zn structure (Chart I), the conformational differences that give rise to this asymmetry are small. In the 4Zn structure, the conformational differences are large: one subunit retains a conformation almost identical with that found in 2Zn–insulin and the other subunit had a large change in the

† Supported by NIH Grant AM 31138 BMT. The 300-MHz NMR spectrometer was purchased under National Science Foundation Instrumentation Grant CHE-82-03497.
‡ Department of Biochemistry.
§ Present address: Spinco Division, Beckman Instruments, Palo Alto, CA 94304.
‖ Department of Chemistry.

0006-2960/88/0427-3387$01.50/0

Chart I: Three-Dimensional Perspective of the 2Zn–Insulin Hexamer Showing Overall Dimensions, Distance between His(B10) Sites (Site I), Location of Ca^{2+} Site (Site II), Arrangement of Subunits, and Details of Metal Ion Coordination[a]

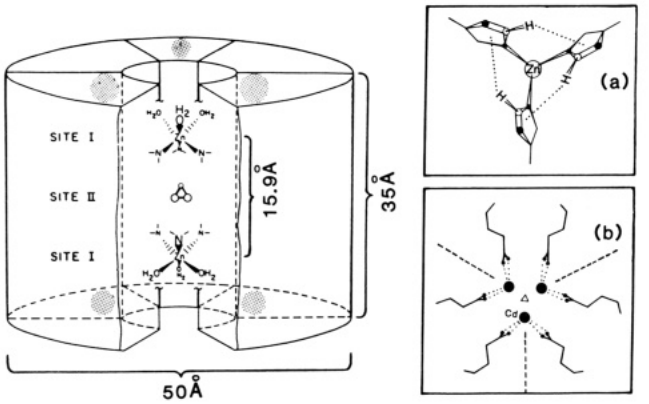

[a] One monomer has been cut away to show the central cavity. The shaded areas indicate the trimer of dimers symmetry. Redrawn from Sudmeier et al. (1981). Inset a shows the propeller-like arrangement of the His(B10) imidazole rings as viewed along the threefold symmetry axis looking out from the hexamer center. This arrangement places the C-2 proton of one ring directly under and directed toward the center of the adjacent ring (● = N). The dotted lines indicate the relationship of each C-2 proton to the adjacent ring. Inset b depicts the structure of the Glu(B13) Ca^{2+} site [as deduced from the X-ray structure of $(In)_6(Cd^{2+})_2Cd^{2+}$; Dunn et al., 1987] viewed along the threefold symmetry axis. Each pair of Glu(B13) carboxylates makes a metal binding site that bridges a dimer–dimer interface (dashed line). The dotted lines indicate the Cd^{2+}–carboxylate bonds. Note that the X-ray structure shows approximately one-third occupancy for each of the three equivalent Cd^{2+} sites (see text).

conformation of the B-chain. A variety of solution and crystal studies show that the interconversion of the 2Zn and 4Zn conformations can be elicited by high concentrations of anions (i.e., Cl^-, I^-, Br^-, or SCN^-) (DeGraaff et al., 1981; Williamson & Williams, 1979; Reinscheidt et al., 1984; Smith et al., 1984). The efficacy with which different anions bring about the 2Zn to 4Zn transition generally follows the Hofmeister lyotropic series, with thiocyanate ion the most effective (DeGraaff et al., 1981).

In the crystalline state, the structural changes associated with the 2Zn to 4Zn transconformation change involve the coordination of zinc, large changes in the conformation of the B-chain, and relatively small changes in the conformation of the A-chain. In 2Zn hexamers, residues 1–8 of the B-chain have an extended conformation, and residues B9–B20 are coiled in an α-helix. In three of the six subunits, the 2Zn to 4Zn transition results in the conversion of residues B1–B8 from the extended conformation to α-helix. This motion brings His(B5) and His(B10) from adjacent subunits close together, creating three new (putative) zinc sites at one end of the hexamer; however, the most recent crystal structure results show these sites are not fully occupied (Smith et al., 1984).

Each zinc in the 2Zn hexamer is coordinated in a distorted octahedral ligand field consisting of three His(B10) imidazolyl groups and three water molecules (Chart I, site I and inset a). These sites are located 15.9 Å apart on the molecular threefold axis in the central water-filled cavity that runs through the hexamer. The four zinc sites of the 4Zn hexamer provide two types of tetrahedral ligand fields: one type involves two solvent molecules (H_2O or an anion) and two histidyls, His(B5) and His(B10); the other type involves three His(B10) histidyls and one solvent molecule (Smith et al., 1984).

A variety of solution and single-crystal diffraction studies provide evidence for a relatively high-affinity Ca^{2+} binding site within the zinc–insulin hexamer (Sudmeier et al., 1981; Storm & Dunn, 1985; Alameda et al., 1985; Kaarsholm & Dunn, 1987; Dunn et al., 1987; C. Hill, Z. Dauter, M. Dunn, and G. Dodson, unpublished results). The ^{113}Cd FT NMR studies of Sudmeier et al. (1981) provided evidence indicating this site (Chart I, site II and inset b) is formed by the convergence of the six Glu(B13) carboxylates in the vicinity of the center of the hexamer [midway between the His(B10) sites].

Several groups have investigated insulin via ^1H NMR (Kowalsky, 1962; Bradbury & Wilairat, 1967; Bradbury & Brown, 1977; Williamson & Williams, 1979; Bradbury et al., 1980; Bradbury & Ramesh, 1985). The work of Williamson and Williams (1979) and Bradbury et al. (1980) is of direct interest to this study; both groups have reported assignments for the histidine C-2 proton region of the zinc–insulin hexamer at pH* 8.9. Williamson and Williams observed a single C-2 resonance at 7.56 ppm for solutions containing insulin and Zn^{2+}; except for small changes in line width, they found no change in the insulin spectrum on going from a ratio of $In:Zn^{2+}$ = 6:1 to a ratio of 6:2, and they found no pH dependence titrating from pH* 8.9 to 8.0. These investigators also reported that integration of the aromatic region of the spectrum gives only *one* histidine C-2 proton. Hence, Williamson and Williams concluded that this resonance must be His(B5) and that the metal-coordinated His(B10) C-2 resonance must be too broad to detect.

Bradbury et al. (1980) reinvestigated the assignments made by Williamson and Williams. They compared the aromatic regions of metal-free bovine insulin and a mutant human insulin, which lacks His(B5), with hagfish insulin, which lacks His(B10). From these comparisons, they were able to assign the C-2 resonance at 7.70 ppm to His(B10) and the resonance at 7.56 ppm to His(B5). In contrast to Williamson and Williams (1979), Bradbury et al. (1980) reported two C-2 histidyl resonances at pH* 9.85 for zinc–insulin ($In:Zn^{2+}$ = 6:2) with chemical shift positions (at 7.68 and 7.54 ppm) nearly identical with those of metal-free insulin at this pH*. Their titration of insulin with Zn^{2+} shows that the downfield resonance (7.68 ppm) appears to decrease in amplitude as the ratio of In:Zn changes from 6:0 to 6:2.1. Nevertheless, from these observations, Bradbury et al. concluded that the binding of Zn^{2+} to His(B10) gives almost *no net change* in the chemical shift of the C-2 proton. They argued that the anticipated deshielding effect of Zn^{2+} (viz., carbonic anhydrase; Campbell et al., 1975) is almost exactly compensated for by an upfield shift due to the protein environment (i.e., ring current anisotropic effects).

Herein, we show that neither of these interpretations is correct. Coordinations of the His(B10) residues, either by Zn^{2+} in the presence of Ca^{2+} or by Cd^{2+}, yields insulin hexamers in which the B10 histidyl C-2 proton resonances are shifted upfield. By coincidence, the C-2 protons of Zn^{2+}-coordinated His(B10) and metal-free His(B5) have essentially the same chemical shift at pH* 9.5–9.9. It will be shown that the relationship between metal ion binding and the chemical shift of the His(B10) C-2 proton resonances is made especially clear both in the Zn^{2+}–Ca^{2+} derivative and in the Cd^{2+} derivative.

To further investigate the metal-binding properties of the Glu(B13) cavity, we have carried out a detailed set of ^1H NMR studies of various metal-substituted insulin hexamers. In this first report, we investigate the effects of Cd^{2+} and Ca^{2+} (in combination with Zn^{2+}) on the histidine C-2 proton region and the aromatic (Phe, Tyr, and His C-4) region of the insulin spectrum as a function of metal ion concentration and pH.

These results are compared with the pH-dependent behavior of the ^{1}H NMR spectrum of $(In)_6(Zn^{2+})_2$.[1]

Experimental Procedures

Materials. ^2H_2O (99.8 atom %, KOR Isotopes), NaO^2H (40% solution in 99+ atom % ^2H_2O, Sigma), ^2HCl (20% solution in 99% atom % ^2H_2O, Sigma), sodium 3-(trimethylsilyl)-1-propanesulfonate-*2,2,3,3-d*$_4$ (Sigma), $ZnSO_4$, $CdSO_4$, $CaCl_2$, and KSCN (Mallinckrodt, analytical reagent grade) were purchased as the highest purity grades available from the indicated sources and used without further purification. Crystalline porcine zinc insulin (containing ~0.5 mol of Zn^{2+}/insulin monomer) was purchased from Elanco Products Co., Eli Lilly and Co., and treated as described below.

Preparation of Metal-Free Insulin. A 10 mg/mL insulin solution was prepared by dissolving crystalline zinc insulin in aqueous pH ~3.0 HCl solution. Zinc ion was removed by extensive dialysis against 1 mM HCl using benzoylated dialysis tubing (Sigma). These metal-free solutions were stored frozen at −15 °C.

Aliquots of the metal-free preparation containing 10–30 mg of insulin were transferred to tared screw-capped vials and lyophilized and then could be stored at room temperature. In this way, a series of samples for the NMR studies could be conveniently prepared by dissolving the lyophilized samples in ^2H_2O.

Determination of Metal Ion and Protein Content. The concentrations of Zn(II) and Cd(II) were assayed spectrophotometrically with a HP 9450A UV–visible spectrophotometer by reaction with 2,2,6-terpyridine (Terpy) by using the following molar extinction coefficients (M^{-1} cm^{-1}): $(Terpy)_2Zn^{2+}$, $\epsilon_{320} = 3.8 \times 10^4$, $\epsilon_{333} = 4.1 \times 10^4$ (Holyer et al., 1966); $(Terpy)_2Cd^{2+}$, $\epsilon_{332} = 3.32 \times 10^4$ (Storm & Dunn, 1985). Via this assay, the "metal-free" insulin prepared as described above typically was found to contain ≤0.002 mol of zinc/insulin monomer. Insulin concentrations were measured spectrophotometrically by using $\epsilon^{1\%}_{277} = 10.6$ ($\epsilon_{277} = 6.04 \times 10^3$ M^{-1} cm^{-1}) in 20 mM phosphate buffer, pH 7.0.

Preparation of NMR Samples. Lyophilized, metal-free insulin was taken up in 1.0 mL of 99.8% ^2H_2O, and the pH* was slowly adjusted by the addition of 0.5 M NaO^2H to ~7.0, where the insulin was just soluble. This solution was allowed to equilibrate overnight at room temperature. Then, the volume was brought to ~1.5 mL, and the pH* was adjusted with 0.5 M NaO^2H to the desired final value. The pH meter readings given herein are uncorrected for the deuterium isotope effect and are indicated as pH* throughout. Depending on the desired final pH*, the combination electrode (Radiometer GK 2322C) was calibrated at either pH 7.00 or pH 10.00 with buffered ^1H_2O standards. For the Cd(II) titration studies, aliquots of 10 mM $CdSO_4$ in ^2H_2O were added at alkaline pH* directly to the insulin sample to give the desired metal/hexamer ratios. However, for titrations with $ZnSO_4$, to avoid sample precipitation, it was necessary to first lower the pH* of the insulin sample to ~3.5 each time prior to adding the metal. Then, the pH* was readjusted to the desired alkaline value.

[1] Abbreviations: In, insulin; $(In)_6(Zn^{2+})_2Ca^{2+}$, the insulin hexamer in which the two His(B10) sites are occupied by Zn^{2+} and the Glu(B13) site is occupied by one Ca^{2+}; $(In)_6(Cd^{2+})_2Cd^{2+}$, the hexamer in which the two His(B10) sites are occupied by Cd^{2+} and the Glu(B13) site is occupied by one Cd^{2+}; $(In)_6(Pb^{2+})_2(Pb^{2+})_3$, the hexamer in which the two His(B10) sites are occupied by Pb^{2+} and the Glu(B13) cavity is occupied by three Pb^{2+} ions; $(In)_6(Zn^{2+})_2$, the hexamer in which Zn^{2+} is coordinated to the His(B10) sites; TSP, sodium 3-(trimethylsilyl)-1-propanesulfonate-*2,2,3,3-d*$_4$; Terpy, 2,2,6-terpyridine; FT, Fourier transform.

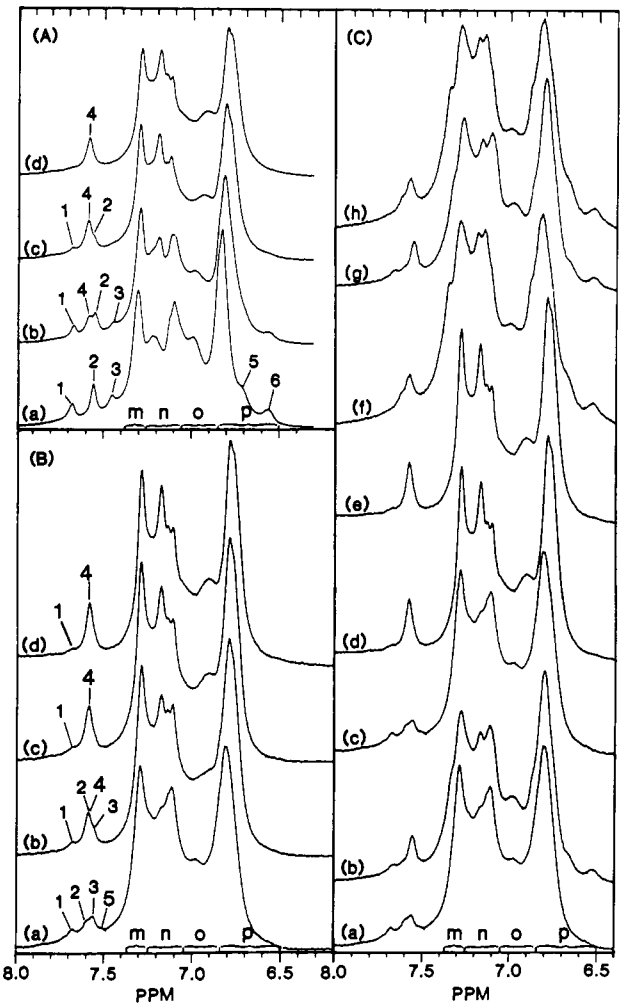

FIGURE 1: Influence of Zn^{2+}, Ca^{2+}, and SCN^- on the aromatic region of the ^{1}H FT NMR spectrum of porcine insulin in ^2H_2O at 25 °C. (A) Titration of insulin with Zn^{2+} in the presence of Ca^{2+} at pH* 9.5. [In]:[Zn^{2+}]:[Ca^{2+}] ratios: (a) 6:0:2; (b) 6:0.7:2; (c) 6:1.4:2; (d) 6:2.1:2. Note that under these conditions, the spectrum of metal-free insulin (a) is unaffected by the presence of Ca^{2+}. Although the [In]:[Ca^{2+}] ratio = 6:2 in this experiment, a ratio of [In]:[Ca^{2+}] = 6:1 causes essentially identical effects (viz., Figure 1B). (B) Titration of zinc–insulin with Ca^{2+} at pH* 9.6. [In]:[Zn^{2+}]:[Ca^{2+}] ratios: (a) 6:2:0; (b) 6:2:0.5; (c) 6:2:1.0; (d) 6:2:2.0. (C) Comparison of the effects of Ca^{2+} and SCN^- on the spectrum of zinc–insulin. Comparisons: $(In)_6(Zn^{2+})_2$ (a) with $(In)_6(Zn^{2+})_2$ plus 50 mM KSCN (b) at pH* 9.6; $(In)_6(Zn^{2+})_2$ (c) with $(In)_6(Zn^{2+})_2Ca^{2+}$ (d) at pH* 9.6; $(In)_6(Zn^{2+})_2Ca^{2+}$ (e) with $(In)_6(Zn^{2+})_2Ca^{2+}$ plus 50 mM KSCN (f) at pH* 9.6; $(In)_6(Zn^{2+})_2$ plus 50 mM KSCN (g) with $(In)_6(Zn^{2+})_2Ca^{2+}$ plus KSCN (h) at pH* 9.5.

^{1}H FT NMR Spectra. The proton NMR spectra were recorded at 300 MHz with a Nicolet NT-300 spectrometer and 1280 computer system. The sample ^2H_2O was used as the field-frequency lock. All spectra were measured at a probe temperature of 22 ± 1 °C. Chemical shifts are reported in parts per million (ppm) downfield from TSP. The signal from residual $^2HO^1H$ in the sample was suppressed with a T^1 inversion–recovery pulse sequence. Most of the spectra shown are the average of 200–400 transients collected over a time period of 20–40 min and accumulated with a repetitive pulse time of ~6 s. Each transient was made up of 8K data points and the spectral width was ±2000 Hz. A 0.5-Hz instrumental line-broadening factor in exponential apodization has been applied to each spectrum. Integration of the histidine C-2 proton region of the spectra was carried out by fitting the signals to Lorenzian line shapes with programs present in the data analysis software of the Nicolet 1280 computer.

RESULTS

In this paper, we are concerned with the assignment of the histidine C-2 region of the spectrum of various insulin hexamers and the characterization of the changes that occur in the aromatic region both when hexamers are formed and when metal ions bind to the Glu(B13) site.

Comparison of Effects of Ca^{2+} and Thiocyanate Ion on the C-2 Region of the ^1H NMR Spectrum of $(In)_6(Zn^{2+})_2$. The aromatic region of the spectrum of metal-free insulin at pH* 9.5 (spectrum a, Figure 1A) is characterized by a broad envelope of resonances extending from 6.5 to 7.4 ppm made up of signals from the aromatic protons of Phe and Tyr and the C-4 protons of His(B5) and His(B10). The C-2 proton resonances of His(B10) and His(B5) in metal-free insulin have been assigned to the signals located at 7.68 (peak 1) and 7.57 ppm (peak 2), respectively (Bradbury et al., 1980). Spectrum a of Figure 1A shows a third resonance in the C-2 region located at 7.43 ppm (peak 3), which has not previously been assigned. We propose that this signal arises from the His(B10) C-2 protons of a higher aggregation state of insulin, probably that of a metal-free tetramer or hexamer. Our studies show that the C-2 region of the spectrum of metal-free insulin is remarkably dependent upon both the pH* and the concentration of insulin. We believe this concentration dependence is due to the presence of various aggregation states of metal-free insulin (i.e., dimer, tetramer, and hexamer). Data consistent with this interpretation will be presented elsewhere (Palmieri, Roy, Lee, and Dunn, unpublished results).

At the concentrations of insulin and Ca^{2+} used to obtain spectrum a of Figure 1A, Ca^{2+} *in the absence of* Zn^{2+} has no influence on the ^1H NMR spectrum of insulin. When Zn^{2+} is added to this Ca^{2+}–insulin sample, there are large changes throughout the aromatic and His C-2 regions of the spectrum (compare spectrum a with spectra b–d of Figure 1A); note that all the resonances in the C-2 region appear to coalesce into one signal (7.58 ppm, peak 4) at this pH*. These changes saturate[2] when the ratio [In]:[Zn^{2+}]:[Ca^{2+}] reaches 6:2:1. The final spectrum (spectrum d) is quite different from the spectrum obtained in the absence of Ca^{2+} (viz., Figure 1B, and compare spectra c and d of Figure 1C).

When Ca^{2+} is titrated into a solution containing insulin and Zn^{2+} (with [In]:[Zn^{2+}] = 6:2) at pH* 9.6 (Figure 1B), the poorly defined, broad resonances in the C-2 region of the zinc–insulin spectrum (peaks 1–3 and 5) coalesce under one signal as the complex with Ca^{2+} is formed (Figure 1B; spectra b–d, peak 4). The residual signal at 7.68 ppm (peak 1) appears to be due to unassembled insulin (see Discussion and Conclusions). The Ca^{2+} effect on the spectrum appears to saturate at a ratio approximating 1 mol of Ca^{2+}/insulin hexamer.[2] The same spectrum is obtained regardless of the order of addition of Ca^{2+} and Zn^{2+}. Consequently, it seems that assembly and dissociation of subunits occurs on a time scale that is rapid relative to the time required for the preparation of the sample and the acquisition of a spectrum.

The SCN^--induced conversion of the 2Zn hexamer to the 4Zn hexamer conformation also brings about large changes in the ^1H NMR spectrum of insulin (Williamson & Williams, 1979). The effects of SCN^- on the spectrum of $(In)_6(Zn^{2+})_2$, both in the presence and in the absence of Ca^{2+}, are shown in spectra a, b, e–g, and h of Figure 1C. Comparison of these spectra indicates that the Ca^{2+} and SCN^- effects are not additive.

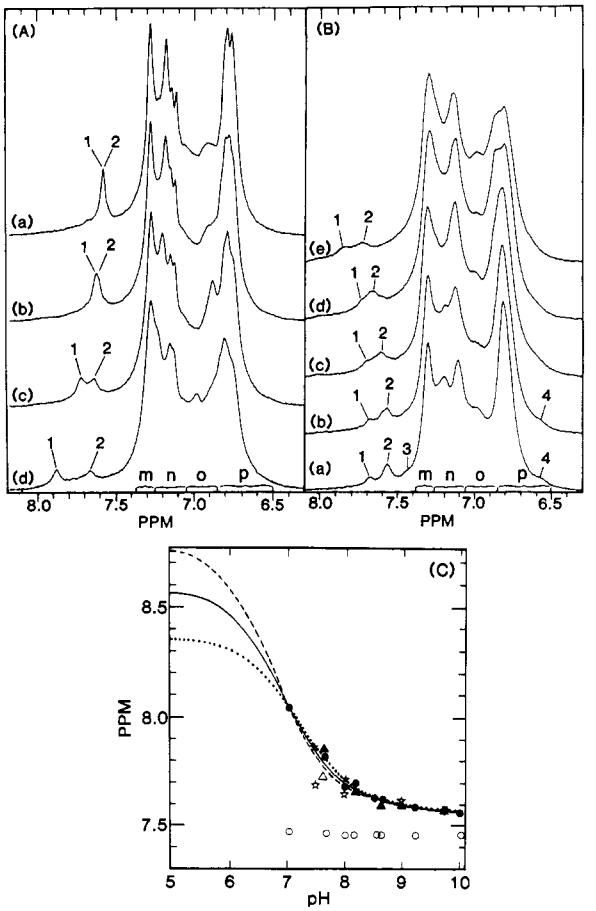

FIGURE 2: Influence of pH* on the aromatic region of the ^1H FT NMR spectra of metal-substituted insulin hexamers. (A) $(In)_6(Zn^{2+})_2Ca^{2+}$. pH values: (a) 9.7; (b) 9.0; (c) 8.0; (d) 7.5. (B) $(In)_6(Zn^{2+})_2$. pH values: (a) 9.7; (b) 9.0; (c) 8.6; (d) 8.1; (e) 7.6. (C) pH* dependencies of the chemical shifts (ppm) of the C-2 resonances of $(In)_6(Zn^{2+})_2Ca^{2+}$ [(★) downfield and (☆) upfield C-2 resonances; points taken from (A)], $(In)_6(Zn^{2+})_2$ [(△) downfield and (▲) upfield C-2 resonances; points taken from (B)], and $(In)_6(Cd^{2+})_2Cd^{2+}$ [(●) downfield and (○) upfield C-2 resonances; points taken from Figure 3B]. The curves drawn through the data points are the best theoretical fits assuming that the shift depends upon an ionization with $pK_a = 7.0$, that proton exchange with solvent is rapid, and that the difference in chemical shift between fully protonated and neutral forms is either 1.0 (—), 1.2 (- - -), or 0.8 ppm (···).

pH Dependence of the C-2 Proton Region of the $(In)_6(Zn^{2+})_2Ca^{2+}$ Spectrum. The titration of Zn^{2+} into a solution of insulin and Ca^{2+} to a final ratio of [In]:[Zn]:[Ca^{2+}] = 6:2.1:2 (spectra a–d of Figure 1A) causes the C-2 proton resonance (peak 1) assigned to His(B10) to move upfield, while His(B5) (peak 2) moves slightly downfield with the result that both resonances exhibit nearly the same chemical shift (peak 4) at pH* 9.5. When the pH is lowered (viz., Figure 2A) this envelope broadens (viz., spectrum b) and then splits into two broad signals (spectra c and d, peaks 1 and 2 of Figure 2A), both of which show some pH* dependence. When the chemical shifts of these resonances are plotted as a function of pH* (see Figure 2C), the resulting curve for the downfield resonance (peak 1) is satisfactorily fitted by assuming that the shift depends upon the ionization of a weak acid with $pK_a \sim 7$ in rapid proton exchange with the solvent and that the difference in chemical shift between fully protonated and neutral forms is 1.0 ± 0.2 ppm, whereas the upfield resonance (peak 2) is

[2] Extension of the titrations shown in Figure 1A, Figure 1C, and Figure 4A to ratios of In:Zn^{2+} = 6:4, In:Ca^{2+} = 6:5, and In:Cd^{2+} = 6:4, respectively, yielded samples with spectra that are characterized by slightly more broadened lines and slightly less metal-free insulin, but otherwise are essentially identical to spectrum d in Figure 1A, Figure 1C, and Figure 3A, respectively. The further addition of metal ions causes these samples to precipitate.

more nearly pH* independent. In the presence of SCN^-, the C-2 proton resonances of $(In)_6(Zn^{2+})_2$ and $(In)_6(Zn^{2+})_2Ca^{2+}$ behave similarly (data not shown).

The C-2 Region of the Spectrum of the Zinc–Insulin Hexamer. In partial agreement with the work of Bradbury et al. (1980), the addition of Zn^{2+} to metal-free insulin at low pH* (pH* ≥ 3) in the ratio $In:Zn^{2+}$ = 6:2 followed by careful titration to the pH* 9.5–9.9 region yields insulin spectra (Figure 2B) that are significantly different from the spectrum of metal-free insulin at the same pH* (compare spectrum a of Figure 1A with spectrum a of Figure 2B). At pH* 9.0, the C-2 region of the spectrum consists of an envelope of at least three broad, overlapping resonances located at ~7.67 (peak 1), 7.56 (peak 2), and 7.43 ppm (peak 3). At pH* 9.7, the histidine C-2 region of the spectrum is characterized by three broad signals, two of low intensity at 7.68 (peak 1) and 7.44 ppm (peak 3) and one of higher intensity at 7.56 ppm (peak 2). *Note that at pH 9.7, the two low-intensity signals, peaks 1 and 2 (at 7.68 and at 7.44 ppm), and the C-2 resonances of metal-free insulin (Figure 1A, trace a, peaks 1–3) occur at virtually the same chemical shifts.* The low-intensity resonance at 6.57 ppm (peak 4 in Figure 2B) present in spectra measured at pH* 8.6 and above (spectra a–c) appears to be characteristic of metal-free insulin (viz., peak 6 of spectrum a in Figure 1A); the presence of this resonance indicates that, under these conditions of pH*, assembly is incomplete. Consequently, we assign the C-2 resonances in the pH* 9.7 spectrum (Figure 2B, spectrum a) at 7.68 (peak 1) and 7.44 peak (peak 3) to metal-free insulin. Under the conditions employed in Figure 2B, when the pH* is lowered below 9.0 (spectra c–e), assembly is more nearly complete. At pH* 8.6 (Figure 2B, spectrum c), a broad envelope of two or more resonances is seen in the C-2 region, and this envelope shifts downfield as the pH* is further decreased (spectrum d). At pH* 7.6, the envelope appears to consist of at least two, partially resolved, broad resonances at 7.84 (peak 1) and 7.72 ppm (peak 2). Due to limitations imposed by the solubility of zinc–insulin, we did not measure spectra below pH* 7.6. The apparent chemical shifts of these two resonances are plotted as a function of pH* in Figure 2C. The resonance located the farthest downfield (peak 1 at pH* 7.6) follows the same pH dependence exhibited by the downfield C-2 proton signal of $(In)_6(Zn^{2+})_2Ca^{2+}$. The upfield signal (peak 2) is also pH dependent. However, the pH dependence of peak 2 appears to be the result of an ionization with a different pK_a*.

The C-2 Region of the Cadmium–Insulin Hexamer Spectrum. The ^{1}H NMR spectra presented in Figure 3A compare the spectrum of metal-free insulin (spectrum a) with the spectra of different ratios of $[In]:[Cd^{2+}]$ at pH* 9.2 (spectra b–d). (Again, note the appearance of four signals, peaks 1–4, in the His C-2 proton region of the spectrum of metal-free insulin at pH* 9.2.) As is evident from comparison of these spectra, the titration of insulin with Cd^{2+} results in significant changes throughout the aromatic region of the spectrum. These changes saturate when the $In:Cd^{2+}$ ratio reaches a value of ~6:3.[2]

The metal ion titration at pH* 9.2 (Figure 3A) shows that as the $[In]:[Cd^{2+}]$ ratio approaches 6:3, the C-2 proton resonances characteristic of metal-free insulin at this pH* value, 7.71 (peak 1), 7.68 (peak 2), 7.57 (peak 3), and 7.47 ppm (peak 4), decrease and that this *decrease* is compensated for by the appearance of two new resonances in the C-2 region at 7.60 (peak 6) and 7.46 ppm (peak 7).

Figure 3B shows the pH dependence of the ^{1}H NMR spectrum of $(In)_6(Cd^{2+})_2Cd^{2+}$ for the pH* range from 10.0

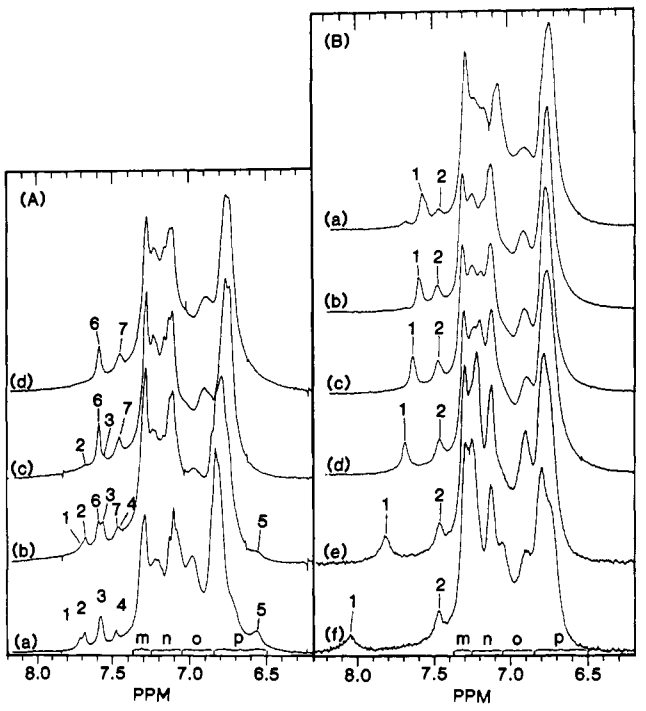

FIGURE 3: Influence of Cd^{2+} and pH* on the aromatic region of the insulin ^{1}H FT NMR spectrum at 25 °C. (A) Titration of metal-free insulin with Cd^{2+} at pH* 9.2 in ^2H_2O. $[In]:[Cd^{2+}]$ ratios: (a) 6:0; (b) 6:1; (c) 6:2; (d) 6:3. (B) Influence of pH* on the spectrum of $(In)_6(Cd^{2+})_2Cd^{2+}$. pH* values: (a) 10.0; (b) 9.2; (c) 8.5; (d) 8.0; (e) 7.65; (f) 7.0. To circumvent solubility problems, for spectra a–d [insulin] = 20 mg/mL and for spectra e and f [insulin] = 3 mg/mL. Control experiments (data not shown) established that the spectrum of $(In)_6(Cd^{2+})_2Cd^{2+}$ at pH* ≥8.0 is unaffected on going from 3 to 20 mg/mL.

to 7.2. Due to the pH-dependent solubility of the hexamer, two different protein concentrations were used (3 mg/mL for the pH* 7.0–8.64 region and 20 mg/mL for the pH* 8.0–10.0 region). The spectra shown in Figure 3B provide evidence indicating that the apparent chemical shift of the downfield C-2 resonance of $(In)_6(Cd^{2+})_2Cd^{2+}$ (peak 1) is pH dependent, shifting from 8.05 ppm at pH* 7.0 to 7.58 ppm at pH* 10.0. The upfield resonance (peak 2) is essentially independent of pH* over this pH* range. At pH* 10.0, the presence of the resonance at 7.68 ppm and the shoulder at 7.45 ppm (peaks 3 and 4 in spectrum a) indicates that, under these experimental conditions, hexamer assembly is incomplete and that traces of metal-free insulin are present.

In Figure 2C, the observed chemical shifts for peaks 1 and 2 of Figure 3B are also plotted as a function of pH. Peak 2 is nearly independent of pH*, whereas peak 1 is clearly dependent on pH*. The theoretical curves, calculated by assuming that the pH dependence arises from a single ionization and that protonation shifts the resonance downfield by 0.8 (dotted line), 1 (solid line), or 1.2 ppm (dashed line), are superimposed on the experimental data for peak 2. These "fits" of the data indicate that the observed pH dependence is consistent with an apparent chemical shift that arises from the protonation of a residue with pK_a* = 7.2 ± 0.5.

Comparison of Effects of Ca^{2+} and Cd^{2+} on the C-2 Region of Insulin Hexamers. Figure 4 compares the ^{1}H NMR spectrum of $(In)_6(Zn^{2+})_2Ca^{2+}$ (spectrum a, pH* 9.5) with the spectra of $(In)_6(Cd^{2+})_2Cd^{2+}$ (spectrum b, pH* 9.2) and $(In)_6(Cd^{2+})_2Ca^{2+}$ (spectra c, pH* 9.8). The differences among these three spectra in the His C-2 region are striking. The resonances assigned to the C-2 proton of His(B10) (peak 2 in each spectrum) clearly are dependent upon the nature of

the metal ion coordinated to the B10 site. As previously remarked, the His(B5) and His(B10) C-2 resonances fall under the same envelope at pH* 9.8. However, the His(B10) resonance is located further upfield in $(In)_6(Cd^{2+})_2Cd^{2+}$ (spectrum b, peak 2) and in $(In)_6(Cd^{2+})_2Ca^{2+}$ (spectrum c, peak 2) than in $(In)_6(Zn^{2+})_2Ca^{2+}$ (spectrum a). It appears that the environment of the C-2 proton of His(B10) is not altered by substitution of Ca^{2+} for Cd^{2+} at the Glu(B13) site (viz., spectra b and c).

Effects of Metal Ion Induced Association on the Aromatic Region of the Insulin ^1H NMR Spectrum. The set of resonances derived from the aromatic rings of the three Phe residues (B1, B24, and B25), the four Tyr residues (A14, A19, B16, and B26), and the C-4 protons of His(B5) and His(B10) undergo interesting shifts induced by the assembly of the zinc and calcium insulin hexamers (viz., Figures 1A and 3A).

For convenience, we subdivide the 6.50–7.40 ppm region into four parts designated regions m–p. In the absence of pronounced anisotropic effects, region m (7.25–7.37 ppm) will be made up of the broad multiplet arising from the aromatic ring Phe protons. Region n (7.05–7.25 ppm) will contain resonances from the 2,6 (meta) protons of Tyr rings. Region o (6.85–7.05 ppm) will contain resonances from the His C-4 protons as well as the 2,6 (meta) protons of some Tyr rings. Region p (6.50–6.85 ppm) will contain resonances from the 3,5 (ortho) protons of the Tyr rings. These subdivisions are based on the ^1H NMR spectra of model peptides where anisotropic effects are small (Wüthrich, 1975; Knowles et al., 1976). Anisotropic effects and/or alterations in ring-flipping rates could cause specific residues to occur either upfield or downfield from these assignments (Wüthrich & Wagner, 1978). Since the aromatic side-chain groups of insulin form clusters along the subunit interfaces, it should be anticipated that anisotropic ring currents and perhaps slow and intermediate ring-flipping rates[3] will combine to cause the ^1H resonances of various of the insulin aromatic residues to occur at chemical shift positions that are considerably diffeent from these idealized values [see Perkins and Wüthrich (1979)].

Titration of Zn^{2+} into insulin samples containing Ca^{2+} (Figure 1A) causes a slight upfield shift in the apparent maximum of the unresolved envelope of resonances in region m (from 7.30 to 7.28 ppm). Region p undergoes a similar upfield shift (from 6.81 to 6.78 ppm). Two new peaks appear, one at 7.17 ppm (region n) and the other at 6.91 ppm (region o); the peak located at 6.97 ppm and the shoulder at 6.55 ppm both disappear.

When Cd^{2+} is titrated into metal-free insulin (Figure 3A), the envelope in region m shifts slightly upfield (from 7.3 to 7.28 ppm) and the envelope in region p shifts from 6.82 to 6.76 ppm. The peak at 6.98 ppm (region o) and the shoulder at 6.55 ppm (region p) both disappear, and a peak at 6.90 ppm (region o) appears. Peaks in the 7.05–7.25 ppm region (region n) change shape, location, and apparent intensity.

In agreement with the X-ray structures of $(In)_6(Zn^{2+})_2$ (Blundell et al., 1972; Baker et al., 1987) and $(In)_6(Cd^{2+})_2Cd^{2+}$

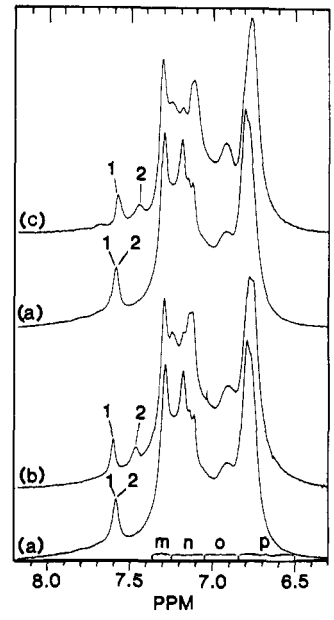

FIGURE 4: Effects of divalent metal ion binding to the Glu(B13) sites of various hexameric insulin derivatives on the aromatic region of the ^1H NMR spectrum at 25 °C in ^2H_2O. Spectra: (a) $(In)_6(Zn^{2+})_2Ca^{2+}$ at pH* 9.5; (b) $(In)_6(Cd^{2+})_2Cd^{2+}$ at pH* 9.2; (c) $(In)_6(Cd^{2+})_2Ca^{2+}$ at pH* 9.5.

(Dunn et al., 1987), the number and nature of the spectral changes that occur during assembly correspond to the large changes in the microenvironments of several of the aromatic side chains as the dimer–dimer interfaces of the hexamer are formed.

Influence of Ca^{2+}, Cd^{2+}, and SCN^- on the Aromatic Region of the Hexamer Spectrum. The interpretation of the spectra presented in Figure 1B is complicated by the finding that the spectrum of the zinc–insulin hexamer (a) is contaminated by the spectrum of metal-free insulin. Consequently, since Ca^{2+} stabilizes the hexamer, the spectral changes brought about by addition of Ca^{2+} are a composite of the changes resulting from the conversion of both $(In)_6(Zn^{2+})_2$ and metal-free insulin to $(In)_6(Zn^{2+})_2Ca^{2+}$. Nevertheless, since the amount of metal-free insulin present at pH* 9.6 is small (we estimate ≤20% of the total insulin subunits present), the observed spectral changes are dominated by the interaction of Ca^{2+} with $(In)_6(Zn^{2+})_2$. At pH* 9.6, these changes include an upfield shift of the peak in region p from 6.81 to 6.78 ppm, the disappearance of a peak at 6.98 ppm and the appearance of the peak at 6.91 ppm in region o, and the appearance of the peak at 7.17 ppm in region n. At lower pH* values, where the assembly of $(In)_6(Zn^{2+})_2$ is more nearly complete, the Ca^{2+} effect can be seen more easily. For example, compare spectrum c of Figure 2A with spectrum d of Figure 2B or spectrum d of Figure 2A with spectrum e of Figure 2B.

Figure 1C compares the effects of Ca^{2+} and SCN^- on the spectrum of $(In)_6(Zn^{2+})_2$. Neither Ca^{2+} nor SCN^- affect the position of the envelope in region m, and the position of the envelope located at 6.81 ppm in $(In)_6(Zn^{2+})_2$ is unaffected by SCN^- (compare spectra a and b). Region n is very sensitive to the interactions of Ca^{2+} and SCN^- with $(In)_6(Zn^{2+})_2Ca^{2+}$. Calcium ion binding shifts the envelope in region p upfield from 6.97 to 6.78 ppm, and the peak at 6.98 ppm (region o of spectra a and b) shifts to 6.91 ppm (viz., spectrum d). When Ca^{2+} and SCN^- are both present, the location of the 6.98 ppm peak is unchanged (spectrum h). The small resonance located at 6.53 ppm (spectra b and f) appears to be a unique signature of the SCN^--induced conformational change. A similar resonance is present in metal-free insulin (Figures 1A and 3A).

[3] When residing in the anisotropic environment of a protein, the individual 2,6 and 3,5 protons of phenylalanine and tyrosine will experience different microenvironments. So long as the ring-flipping rate is rapid relative to the NMR time scale, the chemical shift effects of the anisotropic environment on the symmetry-related 2,6 or 3,5 protons will be averaged out. If ring flipping is slow, then the individual 2,6 or 3,5 protons will each experience different microenvironments that do not average out and, therefore, give different chemical shifts and different splitting patterns. For most proteins at 25 °C, ring-flipping rates are rapid. Bovine pancreatic trypsin inhibitor (Wüthrich & Wagner, 1978) and ferrocytochrome *c* (Campbell et al., 1976) are notable exceptions.

Figure 4 compares the aromatic regions of $(In)_6(Zn^{2+})_2Ca^{2+}$, $(In)_6(Cd^{2+})_2Cd^{2+}$, and $(In)_6(Cd^{2+})_2Ca^{2+}$. Note that the spectra of $(In)_6(Cd^{2+})$ and $(In)_6(Cd^{2+})_2Ca^{2+}$ are highly similar, and in all three derivatives the peak in region m is located at 7.28 ppm and each has a peak at 6.91 ppm. The envelope in region p of $(In)_6(Zn^{2+})_2Ca^{2+}$ (spectrum a or c) is shifted downfield from that of the other two derivatives (6.80 vs 6.77 ppm). The region between 7.05 and 7.25 ppm (region n) is very sensitive to the substitution of Cd^{2+} for Zn^{2+} at the His(B10) sites, but not to the substitution of Cd^{2+} for Ca^{2+} at the Glu(B13) site.

pH Effects on the Aromatic Regions of the $(In)_6(Zn^{2+})_2$, $(In)_6(Zn^{2+})_2Ca^{2+}$, and $(In)_6(Cd^{2+})_2Cd^{2+}$ ^{1}H NMR Spectra.* The spectra presented in Figure 2A show that region m of $(In)_6(Zn^{2+})_2Ca^{2+}$ is insensitive to changes in pH* over the range 9.7–7.5. There are changes throughout the spectrum that result from a broadening of line widths as pH* decreases (compare spectra a and d) and changes in regions n–p from apparent shifts in line positions. The pH*-dependent changes in region o are complicated. A component of the peak located at 6.92 ppm in the pH* 9.7 spectrum (spectrum a) appears to shift upfield and become a shoulder (at ~6.88 ppm) to the Tyr peak at pH* 7.5, and a new peak appears at 6.98 ppm (spectrum d). The positions of peaks at 7.16 and 7.12 ppm are nearly pH* independent; however, the 7.12 ppm peak shifts slightly downfield as pH* decreases. The peak at 7.17 ppm shifts downfield to 7.23 ppm at low pH*. The pH* dependence of this shift is not inconsistent with the assignment of this signal to the C-4 ring protons of His(B5). However, the chemical shift of this resonance is a little too far downfield for an unperturbed His C-4 proton. Alternatively, this pH*-dependent signal could arise from changes in the microenvironment of the Phe(B1) ring as the salt bridge between the α-NH_3^+ of the Phe(B1) and the carboxylate of Glu(A17) is titrated.

The pH* dependence of resonances in the aromatic region of the $(In)_6(Cd^{2+})_2Cd^{2+}$ spectrum is shown in Figure 3B. Again, region m is essentially independent of pH* over the range 9.2–7.0. The envelope at 6.78 ppm (region p of spectrum b) broadens slightly, and the peak position moves downfield to 6.80 ppm as resonances under the envelope move upfield, creating a shoulder at 6.75 ppm at pH* 7.0 (spectrum f). The bandwidth of the peak at 6.90 ppm narrows as pH* decreases, and a new peak appears at 7.05 ppm. The peaks at 7.14 and 7.28 ppm are unaffected by pH* changes in the region 9.2–7.0. However, a shoulder on the 7.12 ppm peak located at 7.19 ppm (spectrum b) shifts downfield as pH* decreases to a value of 7.26 ppm. The pH* dependence of this resonance is similar to that found for the 7.17 ppm resonance of $(In)_6(Zn^{2+})_2Ca^{2+}$ (spectrum a of Figure 2A), and it seems likely that this signal is from either the C-4 proton of His(B5) or the aromatic ring of Phe(B1).

Discussion and Conclusions

The results of previous studies of Cd^{2+} and Ca^{2+} binding to insulin from this laboratory, which employed ^{113}Cd FT NMR spectroscopy, UV–visible spectrophotometry, and equilibrium dialysis (Sudmeier et al., 1981; Storm & Dunn, 1985; Kaarsholm & Dunn, 1987), identified the Glu(B13) cavity of the hexamer as a new binding locus (viz., Chart I). This assignment is confirmed by the X-ray structures of $(In)_6(Cd^{2+})_2Cd^{2+}$ and $(In)_6(Pb^{2+})_2(Pb^{2+})_3$ (Dunn et al., 1987; C. Hill, Z. Dauter, M. F. Dunn, and G. Dodson, unpublished results), which show that in each structure two of the metal ions reside in the His(B10) sites and the remainder in the Glu(B13) cavity (Chart I). In the Cd^{2+} structure, three equivalent but incompletely occupied sites are located within the Glu(B13) cavity, with each site made up of a Glu(B13) pair (Chart I, inset b); in the Pb^{2+} structure, the three Glu(B13) sites are fully occupied. Emdin et al. (1980) have reported X-ray diffraction studies on insulin crystals soaked in Zn^{2+} which show that at relatively high concentrations Zn^{2+} will also bind to the Glu(B13) sites. The equilibrium binding studies of Storm and Dunn (1985) indicate this cavity forms a single high-affinity site for $^{45}Ca^{2+}$. While the biological function of the Ca^{2+} site is not known, the X-ray structure results for the Cd^{2+} and Pb^{2+} derivatives (Dunn et al., 1987) indicate that the binding of Ca^{2+} provides an additional interaction that stabilizes the hexamer by bridging the dimer–dimer interface (Storm & Dunn, 1985). This conclusion is reinforced by a variety of solution kinetic and thermodynamic studies (Dunn et al., 1987; Kaarsholm & Dunn, 1987; Coffman, Fluke, and Dunn, unpublished results).

For the interpretation of the herein described ^{1}H NMR studies, it is our working assumption that there exists a close (but not exact) correspondence between the crystal structures of the 2Zn, 4Zn, and 3Cd hexamers and the solution structures of these species. The X-ray structures[4] define the intramolecular contacts that determine the microenvironments of the aromatic side-chain groups in the crystalline state. It will be shown that changes in the ^{1}H spectrum of *hexameric species* brought about by pH change or metal ion substitution can be explained as due to changes in local electrostatic fields, small changes in the *positions* of the aromatic rings, or possibly changes in ring-flipping rates.[3]

Interpretation of the His C-2 Region. The results derived from analysis of the C-2 region of the ^{1}H NMR spectrum of the insulin derivatives described in this study can be summarized as follows:

(1) The zinc-coordinated His(B10) C-2 proton resonances of $(In)_6(Zn^{2+})_2Ca^{2+}$, both in the presence and in the absence of SCN^-, are shifted upfield relative to metal-free insulin (Figures 1A,C and 2A). In each of these complexes at pH* 9.5–10.0, the C-2 proton resonances of His(B5) and zinc-coordinated His(B10) have nearly the same chemical shift and fall under the same broad signal (viz., spectrum d in Figure 1A, spectrum h of Figure 1C, and spectrum a of Figure 2A). This is also true for $(In)_6(Zn^{2+})_2$ both in the presence and in the absence of 50 mM SCN^- (spectra a and b of Figure 1C and spectrum b of Figure 2B). We propose that the location of the C-2 resonance of Zn^{2+}-coordinated His(B10) is the result of a net upfield shift due to anisotropic ring current effects that involve imidazoyl–imidazoyl interactions (viz., Chart I, inset a) that more than offset a downfield shift due to the deshielding effects of Zn^{2+} coordination [see Perkins and Wüthrich (1979)].

(2) The pH* titrations are consistent with the assignment of a normal pK_a (of ~7) for His(B5) in all hexameric insulin species studied herein (Figure 2C). The pH* dependence to the chemical shift of the C-2 proton resonances of $(In)_6(Zn^{2+})_2$ and $(In)_6(Zn^{2+})_2Ca^{2+}$ could be due to the ionization of a zinc-coordinated water molecule with pK_a >10.

(3) Both Ca^{2+} and SCN^- cause large perturbations of the aromatic region (6.85–7.4 ppm) and smaller perturbations of

[4] It is likely that the asymmetry which gives rise to the observed *approximate* twofold symmetry that relates monomers in the dimeric unit of the hexamer is an artifact of crystal-packing forces (Blundell et al., 1972; Chothia et al., 1983; Baker et al., 1987) and that *in solution* the conformations of monomers within the hexamer are identical, and essentially the same as found in the hagfish dimer X-ray structure (Cutfield et al., 1979, 1981).

the aliphatic region of the spectrum.

(4) Upon coordination to Cd^{2+}, there is a net upfield shift in the position of the C-2 resonance assigned to His(B10) (viz., Figure 3). Coordination to Cd^{2+} renders this resonance pH* independent in the pH* region from 7.0 to 10.0 (Figure 3B).

(5) The lowest field C-2 resonance of $(In)_6(Cd^{2+})_2Cd^{2+}$ at pH* 10.0 shifts further downfield as pH* decreases (peak 1 of Figure 3B), and this pH* dependence can be fit to a $pK_a^* \simeq 7$ (Figure 2C). Accordingly, we assign this pH*-dependent resonance (peak 1 of Figure 3B) to the C-2 proton of His(B5), and we assign the resonance that shifts upfield and becomes pH independent upon coordination to Cd^{2+} (peak 2 of Figure 3B) to the C-2 proton of His(B10).

(6) Under the conditions of concentration used in these studies (3–20 mg/mL, Figure 3A,B), the formation of $(In)_6(Cd^{2+})_2Cd^{2+}$ is essentially complete when insulin and Cd^{2+} are mixed in the ratio 6:3 at pH 9.2 and below.[2] At pH* 10.0, assembly is incomplete (we estimate approximately 80% of the insulin molecules are assembled as hexamer, viz., spectrum a of Figure 3B).

(7) The changes in the spectrum that occur when insulin is titrated either with Zn^{2+} in the presence of Ca^{2+} (Figure 1A) or with Cd^{2+} (Figure 3A) are consistent with an assembly process in which metal-free insulin and either $(In)_6(Zn^{2+})_2Ca^{2+}$ or $(In)_6(Cd^{2+})_2Cd^{2+}$ is the dominant species, respectively, at substoichiometric levels of metal ion. Consequently, it appears that assembly is a positive cooperative process—a conclusion in agreement with previous ^{113}Cd NMR work (Sudmeier et al., 1981), with gel exclusion molecular size studies (Dunn et al., 1980), and with equilibrium dialysis metal binding studies (N. C. Kaarsholm, personal communication).

(8) In the absence of Ca^{2+}, the spectra of zinc–insulin solutions titrated from pH* 9.7 to 7.6 (Figure 2B) show a more complicated pH* dependence for the C-2 proton region. (a) As indicated by the resonances of spectrum a in Figure 2B located at 7.68 (peak 1), 7.44 (peak 3), and 6.57 ppm (peak 4), insulin solutions (20 mg/mL) made up with an [In]:[Zn^{2+}] ratio of 6:2 at high pH* (8.6–9.7) contain significant amounts (perhaps as much as 20%) of metal-free insulin. At lower pH* values (spectra b–e), assembly is more nearly complete. (b) At pH* 9.0–9.7, the effects of Zn^{2+} on the spectrum indicate that the C-2 protons of Zn^{2+}-coordinated His(B10) and His(B5) of the insulin hexamer *have nearly the same chemical shift* (~7.58 ppm; peak 2 of spectrum a in Figure 2B). Consequently, both resonances fall under the same broad envelope (peak 2). (c) As the pH is lowered, the amount of $(In)_6(Zn^{2+})_2$ increases and both of the C-2 resonances that characterize the hexamer shift downfield; however, the shift is greater for peak 1 than for peak 2. At pH* 7.5, these resonances are partially resolved into two broad signals (peaks 1 and 2 of Figure 2B). The dependence of the signal at lower field (peak 1) on pH* is consistent with the protonation of a normal histidine residue with $pK_a^* \simeq 7$ (viz., Figure 2C). We assign this resonance to the C-2 proton of His(B5). The pH* dependence of the signal at higher field (peak 2) appears to depend upon the ionization of a group with a somewhat higher pK_a. We assign peak 2 to the C-2 proton of Zn^{2+}-coordinated His(B10). We speculate that the pH dependence of this resonance arises from the ionization of a water molecule directly coordinated to zinc.

The X-ray structures of $(In)_6(Zn^{2+})_2$ (Dodson et al., 1979, 1980; Baker et al., 1987) and $(In)_6(Cd^{2+})_2Cd^{2+}$ (Dunn et al., 1987; Hill, Dauter, Dodson, and Dunn, unpublished results) show that each His(B10)-coordinated metal ion is coordinated to three water molecules. It is reasonable to expect a pK_a in the range 8–10 for a water molecule directly coordinated to the His(B10) zinc (Dunn, 1975; Woolley, 1975; Billo, 1975; Bertini et al., 1980). Owing to the lower charge density on Cd^{2+}, substitution of Cd^{2+} for Zn^{2+} will increase this intrinsic pK_a by 1–2 pK_a units (Dunn, 1975). Thus, it is likely that the pH* independence of the C-2 resonance assigned to Cd^{2+}-coordinated His(B10) is the consequence of a $pK_a > 10$ for Cd^{2+}-coordinated water.

Contrary to our expectations and to previous assignments (Williamson & Williams, 1979; Bradbury et al., 1980), these studies establish that the net effect of the coordination of either Cd^{2+} or Zn^{2+} to the His(B10) sites within the assembled hexamer is an upfield shift of the C-2 proton resonances of His(B10). We propose that the net upfield shift is due to anisotropic effects contributed by the close proximity of the His(B10) imidazole rings (viz., Chart I, inset a). This ring current effect more than compensates for the expected deshielding effects of metal coordination. Because the deshielding due to metal coordination is less for Cd^{2+} than for Zn^{2+}, the net upfield shift is greater for the Cd^{2+} complex than for the Zn^{2+} complex. The three-dimensional structure of the hexamer (Chart I) is consistent with this explanation.

The incomplete assembly of hexamers at high pH* could be the result of at least three factors. (1) Competition by hydroxide ion for metal ion reduces the amount of free Zn^{2+} available for coordination to the His(B10) sites. (2) Neutralization of the Phe(B1) α-NH_3^+ ion destroys the six salt bridges with Glu(A17) that span the dimer–dimer interfaces and thereby lowers the stability of the hexamer. (3) The X-ray structure of crystalline $(In)_6(Zn^{2+})_2$ indicates that within each dimeric unit the carboxyl groups of the Glu(B13) pairs are hydrogen bonded to each other at pH 6.2. Clearly, at least one carboxyl group of each pair must exist as $-CO_2H$ and therefore has a $pK_a > 6.2$. In the absence of a stabilizing metal ion in the B13 site, the Coulombic effects due to ionization of these carboxyls will also lower the stability of the hexamer. The centrifugation studies of Fredericq (1954, 1956) indicate that the stability of the zinc–insulin hexamer and higher aggregates is substantially decreased at high pH.

In retrospect, it is clear that the inability of earlier groups to correctly assign the His C-2 proton resonances of the zinc–insulin hexamer stems from the fact that most of their hexamer studies were carried out in the pH* region from 8.9 to 9.85, where assembly is incomplete and where the C-2 protons of Zn^{2+}-coordinated His(B10) and (uncoordinated) His(B5) have nearly the same chemical shift. This happenstance, together with a poorly resolved C-2 proton region in $(In)_6(Zn^{2+})_2$ spectra (viz., Figure 2B) and a lack of good information about the pH dependence of the spectrum, made the C-2 region particularly difficult to assign.

Interpretation of Metal Ion Induced Changes in the Aromatic Region. The metal ion induced assembly of the insulin hexamer brings about significant changes in the aromatic region of the spectrum. Both the Phe region (region m) and the Tyr region (region p) shift upfield, and regions n and o undergo considerable change when either $(In)_6(Zn^{2+})_2Ca^{2+}$ or $(In)_6(Cd^{2+})_2Cd^{2+}$ is assembled (viz., Figures 1A and 3A).

Under the conditions of these ^1H NMR studies, metal-free insulin consists of a mixture of insulin dimer and tetramer with small amounts of hexamer in dynamic equilibrium (Pocker & Biswas, 1980; Jeffrey & Coats, 1966; Jeffrey et al., 1976; Strazza et al., 1985; Fredericq, 1954, 1956). Addition of divalent metal ions (such as Zn^{2+} or Cd^{2+}) strongly shifts this equilibrium in favor of hexamer (eq 1–4) (Goldman & Carpenter, 1974; Milthorpe et al., 1977). Therefore, this assembly

$$2(In)_2 \rightleftharpoons (In)_4 \quad (1)$$

$$(In)_2 + (In)_4 \rightleftharpoons (In)_6 \quad (2)$$

$$(In)_6 + 2Zn^{2+} \rightleftharpoons (In)_6(Zn^{2+})_2 \xrightleftharpoons{Ca^{2+}} (In)_6(Zn^{2+})_2Ca^{2+} \quad (3)$$

$$(In)_6 + 3Cd^{2+} \rightleftharpoons (In)_6(Cd^{2+})_2Cd^{2+} \quad (4)$$

process involves a net increase in the number of dimer–dimer interfaces. The 1.5-Å X-ray structure of $(In)_6(Zn^{2+})_2$ (Blundell et al., 1972; Dodson et al., 1979, 1980; Baker et al., 1987) shows that two Phe(B1) and two Tyr(A14) aromatic side chains are brought together in a cluster at each new dimer–dimer interface (Figure 5). At pH 6.2, this cluster is stabilized by a salt bridge involving the α-NH_3^+ of Phe(B1) and the carboxylate of Glu(A17) formed across the dimer–dimer interface. The Phe(B1) ring from one subunit fits into a cleft between the A-chain backbone and the aromatic ring of Tyr(A14) on the adjacent subunit. Although some of the shifts in the aromatic region (m–p) could be due to gross changes in the ring-flipping rate (Wüthrich & Wagner, 1978),[3] it seems highly likely that the shifts are primarily the result of anisotropic ring current effects and changes in environment and/or conformation of the Phe(B1) and Tyr(A14) residues as new dimer–dimer interfaces are assembled. The effects of SCN^- on the hexamer spectrum (compare spectra e and f of Figure 1C) are fully consistent with a change wherein the Phe(B1)-Tyr(A14) cluster (Figure 5) is lost during the transition from the "2Zn structure" to the "4Zn structure". Thus, the shoulder that appears at 7.36 ppm in spectrum f very likely is due to the ring of Phe(B1) in the "4Zn helical conformation", and the changes in regions n and p very likely are due to alteration of the environment of Tyr(A14). Thus, the dominant changes due to assembly of hexamers must have their origins in the new interactions between Phe(B1) and Tyr(A14). Some of the pH*-dependent changes seen in the spectra of $(In)_6(Zn^{2+})_2$, $(In)_6(Cd^{2+})_2Cd^{2+}$, and $(In)_6(Zn^{2+})_2Ca^{2+}$ (Figures 2 and 3) very likely are due to loss of the Phe(B1)-Glu(A17) salt bridge at high pH*.

When Ca^{2+} binds to the Glu(B13) site, the position of the envelope of resonances in region m (the Phe region) is essentially unchanged (Figure 1B). Therefore, we conclude that this insensitivity to the effects of Ca^{2+} binding implies that the microenvironments of the Phe residues that make up this envelope are not significantly altered by Ca^{2+}. Nevertheless, regions n–p show interesting changes (viz., Figure 1B, and compare spectra c and d of Figure 1C and spectrum c of Figure 2A with spectrum e of Figure 2B). Although at present we are unable to assign the resonances that undergo change to specific aromatic side-chain residues, the nature of the spectral perturbations indicates that Ca^{2+} binding induces a conformational change that alters the microenvironment of more than one aromatic residue.[5]

The side chains of Phe(B24), Phe(B25), Tyr(B16), and Tyr(B26) form hydrophobic clusters along the monomer–monomer interface (Figure 6) (Blundell et al., 1972; Dodson et al., 1979, 1980; Baker et al., 1987). One cluster involves two Tyr(B16) residues, two Phe(B24) residues, and two Tyr(B26) residues, which lie against each other at the van der Waals contact distance (4–4.5 Å). The second cluster is formed by the rings of two Phe(B25) residues and one Tyr(A19) ring.[4] The aromatic ring of Phe(B24) from one subunit

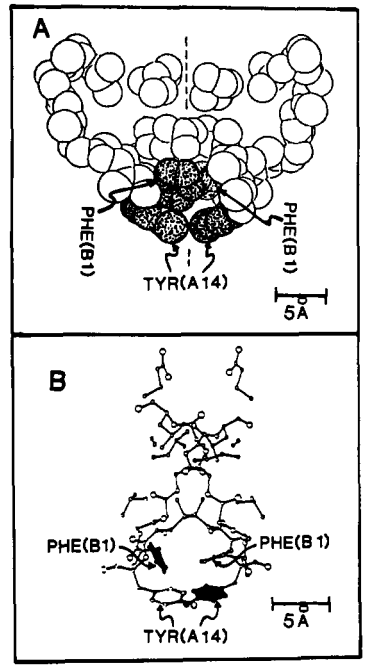

FIGURE 5: (A) Space-filling model of the dimer–dimer interface showing details of the Phe(B1)-Tyr(A14) ring cluster of 2Zn-insulin viewed perpendicular to the twofold axis. The dashed line indicates the location of the interface. (B) The dimer–dimer interface viewed down the threefold axis. The rings of Phe(B1) and Tyr(A14) from one subunit have been darkened. Redrawn from Baker et al. (1987) with permission. Copyright 1987 Royal Society of London.

is packed against the corresponding rings of Phe(B24) and Tyr(B26) from the other subunit, and the two Phe(B25) rings lie against one another on the interface. Phe(B24) and Tyr(B26) are completely shielded from solvent. The hydroxyl of Tyr(B16) is in contact with solvent and is hydrated and the aromatic ring is in a partially nonpolar environment, while the Phe(B25) ring makes contact with solvent.

The crystal structure of $(In)_6(Zn^{2+})_2$ at pH 6.2 shows the Glu(B13) carboxylates arranged in pairs that appear to be hydrogen bonded to each other across the monomer–monomer interface. The crystal structures of $(In)_6(Cd^{2+})_2Cd^{2+}$ and $(In)_6(Pb^{2+})_2(Pb^{2+})_3$ at pH 6.2 show that binding of Cd^{2+} or Pb^{2+} to the Glu(B13) site (viz., Chart I, inset b) establishes new interactions at the introduced metal center across the dimer–dimer interface (Dunn et al., 1987; Hill, Dauter, Dunn, and Dodson, unpublished results). Coordination to the Glu(B13) site involves localized changes in the conformations of the Glu(B13) side chains. We propose that the changes which accompany the binding of Ca^{2+} or Cd^{2+} to the Glu(B13) site must be due to a small change in the conformation of the insulin hexamer, which radiates out along the subunit interfaces and affects some, but not all, of the aromatic residues. Significant changes also are observed in the aliphatic region of the spectrum (data not shown). All these structural changes are probably small. In the 1.9-Å resolution crystal structure of $(In)_6(Cd^{2+})_2Cd^{2+}$ (Dunn et al., 1987), except for Glu(B13), no changes in the positions of side-chain residues were detected. Because the insulin aromatic residues are packed together in hydrophobic clusters, small changes (i.e., <0.2 Å) in ring orientations due to rotations or translations could cause anisotropic ring current changes that result in the observed chemical shifts of the aromatic (and aliphatic) protons. Alternatively, some of the shifts could be caused by changes in ring mobilities from flipping rates that are fast or intermediate (with respect to the NMR time scale) to rates that are slow (Wüthrich & Wagner, 1978).

[5] The α-amino group of Phe(B1) (when neutral) and the carboxylate of Glu(A17) form weak binding sites for Zn^{2+} (Emdin et al., 1980; Kaarsholm & Dunn, 1987) and for Pb^{2+} (C. Hill, Z. Dauter, M. F. Dunn, and G. G. Dodson, unpublished results). Consequently, we cannot rule out the possibility that some of the changes that occur at high pH* upon Ca^{2+} or Cd^{2+} binding are due to interactions at this site.

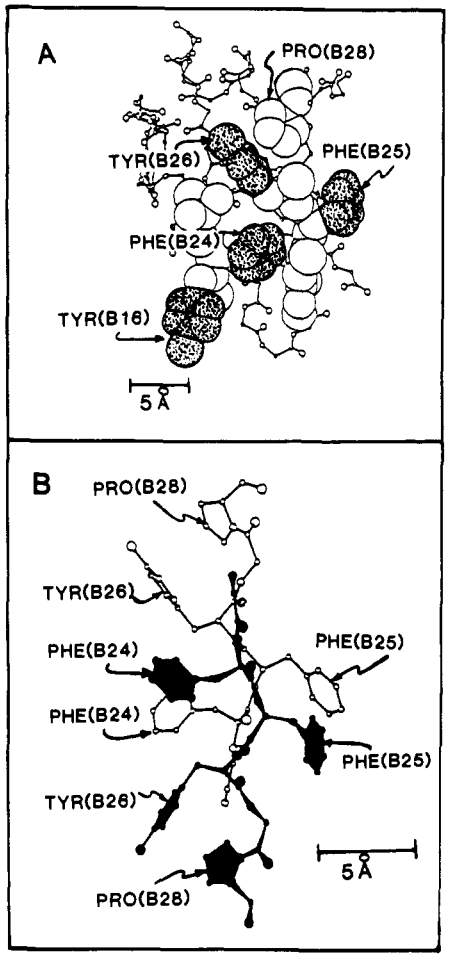

FIGURE 6: (A) Space-filling model of a portion of the insulin monomer showing the locations of Tyr(B16), Phe(B24), Phe(B25), and Tyr(B26) (stippled atoms). The side chains shown in space-filling relief are part of the monomer–monomer interface. (B) Structural detail of the monomer–monomer interface. The interface runs roughly parallel to the plane of the page and passes between the darkened (upper) residues and the lighter residues (below). Redrawn from Baker et al. (1987) with permission. Copyright 1987 Royal Society of London.

Inferred Differences between Hexamers in Solution and in the Crystal. In the crystal, only three of the six insulin subunits undergo the large conformation change during the 2Zn to 4Zn transconformation change (Smith et al., 1984). The NMR studies of Williamson and Williams (1979) and the CD work of Reinscheidt et al. (1984) provide evidence indicating that in solution all six subunits appear to undergo the conformation change. Our own ^{1}H NMR studies of the SCN^- effect are consistent with this interpretation. The His(B5) and His(B10) C-2 protons of hexameric insulins exhibit single broad resonances throughout the pH* range from 7.5 to 9.9. There are no obvious "partial" resonances indicating the presence of more than one form of the hexamer. Consequently, either all six of the subunits undergo the conformation change forming a "6Zn hexamer" structure[6] or all six subunits of the hexamer interconvert between the "2Zn" and "4Zn" conformations (perhaps in a reciprocating fashion) at a rate that is fast relative to the NMR time scale.

The ^{1}H NMR spectra that document the Ca^{2+} effect (Figures 1 and 2) give no evidence for asymmetry either. Again, over the pH* range from 7.5 to 9.9 the C-2 protons of His(B5) and His(B10) each give single broad resonances, and at pH* below 9 there appear to be no obvious partial resonances in the spectrum, thus indicating that a single hexameric species predominates.

[6] The monoclinic crystals of the zinc–insulin hexamer formed in the presence of phenol give a "6Zn–insulin" structure wherein each of the insulin subunits has undergone the large conformation change in which residues B1–B8 assume a helical conformation similar to that found in three of the six subunits of the "4Zn hexamer" structure (G. Dodson and D. Smith, private communication).

ACKNOWLEDGMENTS

We thank Professor Guy Dodson and Dr. Christopher Hill for contributions in the form of suggestions and criticisms of interpretations presented herein and for providing details of the crystalline "6Zn hexamer" structure to us prior to publication.

Registry No. Glu, 56-86-0; thiocyanate, 302-04-5.

REFERENCES

Alameda, G. K., Evelhoch, J. L., Sudmeier, J. L., & Birge, R. R. (1985) *Biochemistry 24*, 1757–1762.

Andersen, T., & Berggren, P.-O. (1979) *Acta Endocrinol. (Copenhagen), Suppl. S277*, 8.

Baker, E. N., Blundell, T. L., Cutfield, J. F., Cutfield, S. M., Dodson, E. J., Dodson, G. G., Hodgkin, D. C., Hubbard, R. E., Isaacs, N. W., Reynolds, C. D., Sakabe, K., Sakabe, N., & Vijayan, N. M. (1987) *Phil. Trans. R. Soc. London, Ser. B* (in press).

Bentley, G. A., Dodson, E. J., Dodson, G. G., Hodgkin, D. C., & Mercola, D. A. (1976) *Nature (London) 261*, 166–168.

Bertini, I., Canti, G., Luchinat, C., & Mani, F. (1980) *Inorg. Chim. Acta 46*, 291.

Bi, R. C., Dauter, Z., Dodson, E., Dodson, G., Giordano, F., & Reynolds, C. (1984) *Biopolymers 23*, 391–395.

Billo, E. J. (1975) *Inorg. Nucl. Chem. Lett. 11*, 491.

Blundell, T., Dodson, G., Hodgkin, D., & Mercola, D. (1972) *Adv. Protein Chem. 26*, 279–402.

Bradbury, J. H., & Wilairat, P. (1967) *Biochem. Biophys. Res. Commun. 29*, 84–89.

Bradbury, J. H., & Brown, L. R. (1977) *Eur. J. Biochem. 76*, 573–582.

Bradbury, J. H., & Ramesh, V. (1985) *Biochem. J. 229*, 731–737.

Bradbury, J. H., Ramesh, V., & Dodson, G. (1980) *J. Mol. Biol. 150*, 609–613.

Campbell, I. D., Dobson, C. M., & Williams, R. J. P. (1975) *Proc. R. Soc. London, B 189*, 503–509.

Campbell, I. D., Dobson, C. M., Moore, G. R., Perkins, S. J., & Williams, R. J. P. (1976) *FEBS Lett. 70*, 96–100.

Chothia, C., Lesk, A. M., Dodson, G. G., & Hodgkin, D. C. (1983) *Nature (London) 302*, 500–505.

Cutfield, J. F., Cutfield, S. M., Dodson, E. J., Dodson, G. G., Emdin, S. O., & Reynolds, C. D. (1979) *J. Mol. Biol. 132*, 85–100.

Cutfield, J. F., Cutfield, S. M., Dodson, E. J., Dodson, G. G., Reynolds, C. D., & Vallely, D. (1981) in *Structural Studies on Molecules of Biological Interest* (Dodson, G., Glusker, J. P., & Sayre, D., Eds.) p 527, Clarendon and Oxford University Press, London.

De Graaff, R. A. G., Lewit-Bentley, A., & Tolley, S. P. (1981) in *Structural Studies on Molecules of Biological Interest* (Dodson, G., Glusker, J. P., & Sayre, D., Eds.) pp 547–556, Clarendon and Oxford University Press, London.

Dodson, E. J., Dodson, G. G., & Hodgkin, D. C. (1979) *Can. J. Biochem. 57*, 469–479.

Dodson, E. J., Dodson, G. G., & Hodgkin, D. C. (1980) in *Frontiers of Bioinorganic Chemistry and Molecular Biology* (Anachenko, A. N., Ed.) p 145, Pergamon, Oxford.

Dong-Cai, L., Jin-Bi, D., Stuart, D., Zhu-Li, W., Todd, R., Jun-Ming, Y., & Mei-Zhen, L. (1983) *Biochem. Soc. Trans. 11*, 419–425.

Dunn, M. F. (1975) *Struct. Bonding (Berlin) 23*, 61–122.

Dunn, M. F., Pattison, S. E., Storm, M. C., & Quiel, E. (1980) *Biochemistry 19*, 718–725.

Dunn, M. F., Palmieri, R., Kaarsholm, N. C., Roy, M., Lee, R., Dauter, Z., Hill, C., & Dodson, G. G. (1987) in *Proceedings of the Fifth International Symposium on Calcium Binding Proteins in Health and Disease* (Norman, A. W., Vanaman, T. C., & Means, A., Eds.) pp 372–383, Academic, New York.

Emdin, S. O., Dodson, G., Cutfield, J. M., & Cutfield, S. M. (1980) *Diabetologia 19*, 174–182.

Fredericq, E. (1954) *J. Polym. Sci. 12*, 287–300.

Fredericq, E. (1956) *Arch. Biochem. Biophys. 65*, 218–228.

Goldman, J., & Carpenter, F. H. (1974) *Biochemistry 13*, 4566–4574.

Greider, M. H., Howell, S. L., & Lacy, P. E. (1969) *J. Cell Biol. 41*, 162–166.

Hellman, B., Sehlin, J., & Täljedal, L.-B. (1976) *Science (Washington, D.C.) 194*, 1421.

Howell, S. L. (1974) *Adv. Cytopharmacol. 2*, 319.

Howell, S. L., Tyhurst, M., Duvefelt, H., Andersson, A., & Hellerstrom, C. (1978) *Cell Tissue Res. 188*, 107.

Jeffrey, P. D., & Coates, J. H. (1966) *Biochemistry 5*, 3820–3824.

Jeffrey, P. D., Milthorpe, B. K., & Nichol, L. W. (1976) *Biochemistry 15*, 4660–4665.

Kaarsholm, N. C., & Dunn, M. F. (1987) *Biochemistry 26*, 883–890.

Knowles, P. F., Marsh, D., & Rattle, H. W. E. (1976) *Magnetic Resonance of Biomolecules*, pp 110–146, Wiley, New York.

Kowalsky, A. (1962) *J. Biol. Chem. 237*, 1807–1819.

Lacy, P. E. (1957) *Diabetes 6*, 498.

Milthorpe, B. K., Nickel, L. W., & Jeffrey, P. D. (1977) *Biochim. Biophys. Acta 495*, 174–202.

Peking Insulin Structure Research Group (1974) *Sci. Sin. (Engl. Ed.) 17*, 779–792.

Perkins, S. J., & Wüthrich, K. (1979) *Biochim. Biophys. Acta 576*, 409–423.

Pocker, Y., & Biswas, S. B. (1980) *Biochemistry 19*, 5043–5049.

Pocker, Y., & Biswas, S. B. (1981) *Biochemistry 20*, 4354–4361.

Reinscheidt, H., Strassburger, W., Glatter, U., Wollmer, A., Dodson, G. G., & Mercola, D. A. (1984) *Eur. J. Biochem. 142*, 7–14.

Sakabe, N., Sakabe, K., & Sasaki, K. (1981) in *Structural Studies on Molecules of Biological Interest* (Dodson, G., Glusker, J. P., & Sayre, D., Eds.) pp 509–526, Clarendon and Oxford University Press, London.

Smith, G. D., Swenson, D. C., Dodson, E. J., Dodson, G. G., & Reynolds, C. D. (1984) *Proc. Natl. Acad. Sci. U.S.A. 81*, 7093–7097.

Storm, M. C., & Dunn, M. F. (1985) *Biochemistry 24*, 1749–1756.

Strazza, S., Hunter, R., Walker, E., & Darnall, D. W. (1985) *Arch. Biochem. Biophys. 238*, 30–42.

Sudmeier, J. L., Bell, S. J., Storm, M. C., & Dunn, M. F. (1981) *Science (Washington, D.C.) 212*, 560–562.

Williamson, K. L., & Williams, R. J. P. (1979) *Biochemistry 18*, 5966–5972.

Woolley, P. (1975) *Nature (London) 258*, 675, 677–682.

Wüthrich, K. (1975) *NMR in Biological Research: Peptides and Proteins*, pp 42–118, North-Holland and American Elsevier, New York.

Wüthrich, K., & Wagner, G. (1978) *Trends Biochem. Sci. (Pers. Ed.) 3*, 227–230.